Additional work is underway to improve the accuracy and extend the frequency range of the current measurement system. More sophisticated sample holder modeling techniques are being investigated in order to enhance the accuracy of the permittivity measurements. Another point being examined is the possibility of deriving $\hat{\epsilon}$ of a solution by using the differential plot and a knowledge of $\hat{\epsilon}$ of the solvent, since this procedure seems insensitive to many of the error mechanisms. The system is also being reconfigured to provide an automated power-sweep capability to enable fixed-frequency power domain measurements. Further experimental work is directed toward identifying and quantifying any (narrow-band?) frequency and/or power-specific responses in complex chemical and biological systems. Ultimately, it is hoped that the information obtained in this manner will be useful not only in fundamental studies of dielectric properties but also in the design of biological experiments which involve responses that may have frequency or field strength dependencies.

ACKNOWLEDGMENT

Thanks are due R. Baudendistel and W. Parrot for assistance in the construction of several components. The help of Barbara Sinha in preparing the sample solutions is appreciated. The authors also wish to thank Dr. W. T. Joines for valuable discussions.

REFERENCES

[1] S. M. Bawin, L. K. Kaczmarek, and W. R. Adey, "Effects of mediated VHF fields on the central nervous system," in *Biologic Effects of Nonionizing Radiation, Ann. N.Y. Acad. Sci.*, vol. 247, pp. 74–81, Feb. 1975.

[2] C. F. Blackman, J. A. Elder, C. M. Weil, S. G. Benane, D. C. Eichinger, and D. E. House, "Induction of calcium-ion efflux from brain tissue by radio-frequency radiation: Effects of modulation frequency and field strength," Special Supplement, Biological Effects of Electromagnetic Waves, *Radio Sci.*, 1979.

[3] C. E. Tinney, J. L. Lords, and C. H. Durney, "Rate effects in isolated turtle hearts induced by microwave irradiation," *IEEE Trans. Microwave Theory Tech.*, vol. MTT-24, pp. 18–24, Jan. 1976.

[4] S. M. Bawin, A. Sheppard, and W. R. Adey, "Possible mechanisms of weak electromagnetic field coupling in brain tissue," *Bioelectrochem. Bioenergetics*, vol. 5, pp. 67–76, 1978.

[5] M. L. Swicord, "Broadband measurements of dielectric properties," in *Proc. Symp. Biological Effects and Measurement of Radio Frequency/Microwaves*, HEW publication (FDA) 77-8026, Rockville, MD, July 1977.

[6] E. H. Grant, R. J. Sheppard, and G. P. South, *Dielectric Behaviour of Biological Molecules in Solution*. Oxford, England: Clarendon Press, 1978.

[7] H. Fellner-Feldegg, "A thin-sample method for the measurement of permeability, permittivity, and conductivity in the frequency and time domain," *J. Phys. Chem.*, vol. 76, no. 15, pp. 2116–2123, 1972.

[8] A. H. Clark, P. A. Quickenden, and A. Suggett, "Multiple reflection time domain spectroscopy," *J. Chem. Soc. Faraday Trans. II*, vol. 70, pp. 1847–1861, 1974.

[9] C. P. Lawinski, J. C. W. Shepherd, and E. H. Grant, "Measurement of permittivity of solution of small biological molecules at radiowave and microwave frequencies," *J. Microwave Power*, vol. 10, pp. 147–162, July 1975.

[10] Hewlett Packard Co. Application Note 183, "High frequency swept measurements," Nov. 1977

[11] H. E. Green, "The numerical solution of some important transmission-line problems," *IEEE Trans. Microwave Theory Tech.*, vol. MTT-13, pp. 676–692, 1965.

[12] H. P. Schwan, R. J. Sheppard, and E. H. Grant, "Complex permittivity of water at 25°C," *J. Chem. Phys.*, vol. 64, pp. 2257–2258, 1976.

[13] A. R. von Hippel, Ed., *Dielectric Materials and Applications*. Cambridge, MA: MIT Press, 1954, p. 361.

Irradiation of Prolate Spheroidal Models of Humans in the Near Field of a Short Electric Dipole

MAGDY F. ISKANDER, MEMBER, IEEE, PETER W. BARBER, MEMBER, IEEE, CARL H. DURNEY, MEMBER, IEEE, AND HABIB MASSOUDI, MEMBER, IEEE

***Abstract*—Analysis of the near-field irradiation of prolate spheroidal models of humans and animals by a short electrical dipole is described. The method of solution involves an integral equation formulation of the problem in terms of the transverse dyadic Green's function and expanding the fields irradiated by a short dipole in terms of the vector spherical harmonics. The extended boundary condition method (EBCM) is employed to solve the integral equations. The power distribution and the average specific absorption rate (SAR) are calculated and plotted as a function of the separation distance. It is shown that for a dipole placed along the major axis of the spheroidal (k-polarization [1]), and for a very short separation distance, $d = 0.15\ \lambda$, the relative power values at both ends of the spheroid are about 40 compared with the ratio of 15 in the planewave exposure case. Furthermore, the calculated average SAR values**

Manuscript received September 14, 1979; revised January 24, 1980.

The authors are with the Department of Electrical Engineering, University of Utah, Salt Lake City, UT 84112.

0018-9480/80/0700-0801$00.75 ©1980 IEEE

as a function of the separation distance were found to oscillate around the constant value obtained from the planewave irradiation case. Differences between the near- and far-field exposure cases occurred only at separation distances shorter than 0.5 λ where the magnitudes of the electric and magnetic energy densities are higher than the time-average radiation power density.

I. Introduction

THE FAMILIAR concept of expressing electromagnetic energy absorption in biological models in terms of average power density is only satisfactory for planewave irradiation [1]–[6]. Although calculations based on far-field (planewave) irradiation have been valuable in many practical applications and have led to a better understanding of the nature of the interaction between electromagnetic fields and biological objects, it is more realistic to consider near-field illumination. This is because many industrial and medical applications utilize radio frequency sources operating at lower frequencies, and therefore the exposures are occurring in the near field and their effects cannot be adequately explained in terms of planewave results. The medical therapeutic treatments [7] and the industrial applications at 27 MHz [8], [9] (which is allocated by the Federal Communications Commission for industrial, medical, and scientific applications) are typical examples where electromagnetic power sources are used at lower frequencies. Furthermore, it is believed that some biological effects occurring at low power levels (<500 μW) are due to the concentration of thermalized energy—hot spots—which may conspire to product thermal stimulation [10]. It is, therefore, of particular interest to investigate the effect of the reactive energy components on the SAR distribution and average SAR in human and animal models. Because of the complications associated with defining, calculating, or measuring the near-field radiation, problems associated with near-field irradiation of biological models have not been solved.

In this paper a solution of the near-field irradiation of prolate spheroidal models by an electrically short dipole is presented. The prolate spheroidal model is used since, for the planewave irradiation case, it was found to give an estimate of the average specific absorption rate (SAR) which agrees very well with those obtained from more realistic but complicated models [1]. Furthermore, the near-field radiation from a short dipole can be calculated exactly and hence used to identify and establish the suitable field parameters necessary to quantify the hazardous level of electromagnetic radiation.

II. Formulation

Consider a prolate spheroidal model irradiated by a short dipole located at an arbitrary point $\bar{r}'$ as shown in Fig. 1. By using the equivalence principle, the induced fields in the spheroid can be replaced by equivalent electric and magnetic surface current densities [5]. The electromagnetic field problem can then be solved by employing an integral formulation involving these surface currents and equating the total field to zero throughout

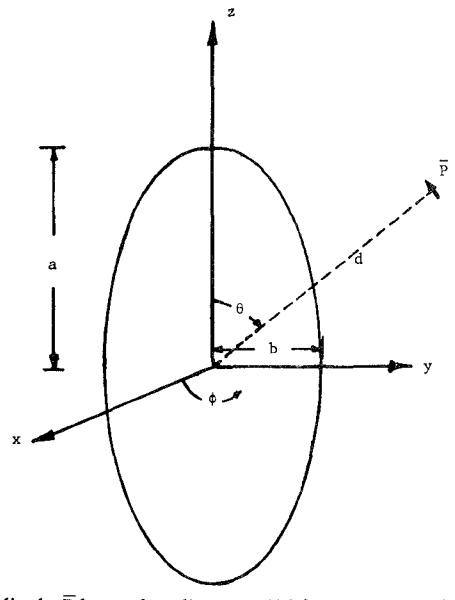

Fig. 1. A dipole $\bar{P}$ located at distance $\bar{r}'(d,\theta,\phi)$ from a prolate spheroid model of man.

the interior volume of the spheroid [10], [11]. By applying the boundary condition at the surface, it can be shown that the internal field can be obtained from [5]:

$$\nabla\times\int_s(\bar{n}\times\bar{E})\cdot\bar{G}(k\bar{r}|k\bar{r}')\,ds$$

$$-\nabla\times\nabla\times\int_s\frac{1}{j\omega\epsilon_0}(\bar{n}\times\bar{H})\cdot\bar{G}(k\bar{r}|k\bar{r}')\,ds=-\bar{E}^i_{\text{dip}}(\bar{r},\bar{r}') \quad (1)$$

where $\bar{n}\times\bar{E}$ and $\bar{n}\times\bar{H}$ are the equivalent magnetic and electric surface current densities, respectively. $\bar{E}^i_{\text{dip}}(\bar{r},\bar{r}')$ is the incident field from a short dipole and $\bar{G}(k\bar{r}|k\bar{r}')$ is the transverse dyadic Green's function given by

$$\bar{G}(k\bar{r}|k\bar{r}')=jk\sum_l\sum_{m=-l}^{l}\left[\left\{h_l(kr')\bar{X}_{lm}\right\}\cdot\left\{j_l(kr)\bar{X}_{lm}\right\}\right.$$

$$\left.+\frac{1}{k^2}\nabla\times\left\{h_l(kr')\bar{X}_{lm}\right\}\cdot\nabla\times\left\{j_l(kr)\bar{X}_{lm}\right\}\right] \quad (2)$$

where $h_l(x)$ and $j_l(x)$ are the spherical Hankel and Bessel functions, respectively, and $\bar{X}_{lm}$ are the vector spherical harmonics [12].

$$\bar{X}_{lm}(\theta,\phi)=\frac{1}{\sqrt{l(l+1)}}\bar{L}Y_{lm}(\theta,\phi) \quad (3)$$

where $\bar{L}=-j(\bar{r}\times\nabla)$ and

$$Y_{lm}(\theta,\phi)=\sqrt{\frac{(2l+1)(l-m)!}{4\pi(l+m)!}}\;P_l^m(\cos\theta)e^{jm\phi}.$$

To reduce (1) to a system of simultaneous equations, it is necessary to expand the internal and incident fields in terms of the vector spherical harmonics and apply the orthogonality properties of these functions. The internal fields can be easily expanded in terms of the vector spherical harmonics with the unknown expansion coefficients to be determined using the EBCM. The elec-

tric field irradiated by a short dipole, on the other hand, can be easily found in terms of the spherical harmonics [12], [13]. To reduce (1) to a system of integral equations, however, it is required to expand the dipole fields in terms of the spherical vector harmonics and use the orthogonality properties of these functions. For a short dipole with dipole moment $\bar{P}$, it can be shown [14] that the radiated electric field is given by

$$\bar{E}^i_{\text{dip}}(\bar{r},\bar{r}') = \frac{1}{4\pi\epsilon_0}\sum_l \sum_{m=-l}^{l} \frac{j}{k} a_E(l,m)\nabla\times\{j_l(kr)\bar{X}_{lm}(\theta,\phi)\} + a_M(l,m)\{j_l(kr)\bar{X}_{lm}(\theta,\phi)\} \quad (4)$$

where the spherical Bessel functions have been chosen since the dipole lies outside the spheroid and $a_E(l,m)$ and $a_M(l,m)$ are the expansion coefficients given by

$$a_E(l,m) = \frac{2\pi jk^3}{\sqrt{l(l+1)(2l+1)}} \bar{P}\cdot\left[\frac{(l+1)h_{l-1}(kr')}{\sqrt{(2l-1)}}\bar{\epsilon}^- + \frac{lh_{l+1}(kr')}{\sqrt{(2l+3)}}\bar{\epsilon}^+\right] \quad (5)$$

$$\epsilon_x^- = [(l+m)(l+m-1)]^{1/2} Y^*_{l-1,m-1}(\bar{r}') - [(l-m)(l-m-1)]^{1/2} Y^*_{l-1,m+1}(\bar{r}')$$

$$\epsilon_y^- = -j\{[(l+m)(l+m-1)]^{1/2} Y^*_{l-1,m-1}(\bar{r}') + [(l-m)(l-m-1)]^{1/2}\cdot Y^*_{l-1,m+1}(\bar{r}')\}$$

$$\epsilon_z^- = -2[(l+m)(l-m)]^{1/2} Y^*_{l-1,m}(\bar{r}')$$

$$\epsilon_x^+ = [(l+m+1)(l+m+2)]^{1/2} Y^*_{l+1,m+1}(\bar{r}') - [(l-m+1)(l-m+2)]^{1/2} Y^*_{l+1,m-1}(\bar{r}')$$

$$\epsilon_y^+ = j\{[(l+m+1)(l+m+2)]^{1/2} Y^*_{l+1,m+1}(\bar{r}') + [(l-m+1)(l-m+2)]^{1/2} Y^*_{l+1,m-1}(\bar{r}')\}$$

$$\epsilon_z^+ = -2[(l+m+1)(l-m+1)]^{1/2} Y^*_{l+1,m}(\bar{r}')$$

and

$$a_M(l,m) = \frac{2\pi jk^3 h_l(k\bar{r}')\bar{P}\cdot\bar{M}}{\sqrt{l(l+1)}} \quad (6)$$

where

$$M_x = [(l-m)(l+m+1)]^{1/2} Y^*_{l,m+1}(\bar{r}') + [(l+m)(l-m+1)]^{1/2} Y^*_{l,m-1}(\bar{r}')$$

$$M_y = [(l-m)(l+m+1)]^{1/2} Y^*_{l,m+1}(\bar{r}') - [(l+m)(l-m+1)]^{1/2} Y^*_{l,m-1}(\bar{r}')$$

$$M_z = 2mY^*_{lm}(\bar{r}').$$

By substituting (2) and (4) in (1) and using the orthogonality properties of the vector spherical harmonics, (1) reduces to

$$jk\left[\int_s (\bar{n}\times\bar{E})\times\nabla\times(h_l(kr')\bar{X}_{lm}) + j\sqrt{\frac{\mu_0}{\epsilon_0}}\, k(\bar{n}\times\bar{H})\cdot(h_l(kr')\bar{X}_{lm})\right] ds = -\frac{1}{4\pi\epsilon_0} a_M \quad (7)$$

$$k\left[\int_s (\bar{n}\cdot\bar{E})\cdot k(h_l(kr')\bar{X}_{lm}) + j\sqrt{\frac{\mu_0}{\epsilon_0}}\, (\bar{n}\times\bar{H})\cdot\nabla\times(h_l(kr')\bar{X}_{lm})\right] ds = -\frac{1}{4\pi\epsilon_0} a_E. \quad (8)$$

The internal electric fields can be expanded in terms of the vector spherical harmonics in the form:

$$\bar{E} = \sum_l \sum_m C_{lm}(j_l(kr)\bar{X}_{lm}) + D_{lm}\nabla\times(j_l(kr)\bar{X}_{lm}). \quad (9)$$

Hence by using the orthogonality properties of $(h_l(kr')\bar{X}_{lm})$ and $\nabla\times(h_l(kr')\bar{X}_{lm})$, (7) and (8) reduce to two sets of infinite simultaneous equations in the unknown expansion coefficients. It should be noted that (7) and (8) are similar to those derived in [5] with the exception that the function $\bar{X}_{lm}$ is to be calculated for $-l<m<l$ instead of acquiring only positive numbers as in the case in [15]. Furthermore, since the function $\bar{X}_{lm}$ involves an exponential term in ϕ, (7) and (8) can be further expressed in terms of four equations, each involving either an even or odd function of ϕ.

III. Numerical Procedure and Results

For a dipole of arbitrary location and orientation, the incident field expansion in (4) should be programmed and used in (1). However, considerable simplification can be derived if the dipole location is restricted to specific locations of interest. For example, if the dipole is assumed to be located at the $\phi=0$ plane, the terms involving $\sin m\phi$ in (5)–(8) are zero. This assumption does not limit the generality of the problem since the prolate spheroidal model is symmetrical around the z axis and hence the calculations will be the same regardless of the specific constant ϕ plane used. Also if θ is given the values 180° and 90°, considerable simplification in calculating the spherical harmonics can be achieved. These specific values of θ are chosen to correspond to the k polarization and the E or H polarization, respectively, for the plane-wave incidence cases [1]–[5].

For these specific cases of interest, a computer program to solve (1) on the UNIVAC 1108 computer was written and results are given below. Consider first the case where the dipole is placed on the $\phi=0$ plane and at $\theta=180°$. This corresponds to the k-polarization case for an incident planewave. In this case it can be shown that the expansion coefficients $a_E(l,m)$ and $a_M(l,m)$ are only different from zero for $m=0,\pm1$. Furthermore, if the dipole moment is assumed to be lying in the x–y plane, i.e., $\bar{P}(P_x,P_y,0)$, only the $m=\pm1$ terms will remain. To check the accuracy of the numerical procedure, comparison was made be-

TABLE I
COMPARISON BETWEEN THE PLANEWAVE (k-POLARIZATION [1]) SAR DISTRIBUTION IN A SPHEROIDAL MODEL OF MAN ($a=0.875$ m AND $a/b=6.134$) AT 27 MHz AND THE CORRESPONDING VALUES OBTAINED WHEN THE SAME MODEL IS IRRADIATED BY THE FIELDS OF A SHORT ELECTRIC DIPOLE OF MOMENT IN THE x-DIRECTION $\bar{P}=\bar{P}_x$ AND LOCATED AT $\theta=\pi$ AND DISTANCE $d=2\lambda$

Point Location (r, θ, φ)	SAR (W/kg)	
	Plane Wave	Short Electric Dipole
(a, 0, 0)	4.56×10^{-5}	4.39×10^{-5}
(b, π/2, 0)	9.71×10^{-3}	9.75×10^{-3}
(b, π/2, π/2)	8.45×10^{-5}	8.05×10^{-5}
(a/2, π, 0)	3.28×10^{-4}	3.29×10^{-4}
(a, π, 0)	5.88×10^{-4}	6.17×10^{-4}

tween the SAR distribution in a spheroidal model of man when irradiated by the fields of a dipole located at a large separation distance $d=2\lambda$ from the center of the spheroid and when exposed to the planewave radiation, k-polarization case [1]. These SAR distribution values are given in Table I where it is clear that the results from both cases are in good agreement. It should be noted that the spheroidal model of man has the dimensions of $a=0.875$ m and $a/b=6.34$, and of complex permittivity equal to 2/3 that of the muscle tissue, i.e., $\epsilon'=78.5$ and $\epsilon''=270$ at 27 MHz [1]. Furthermore, the value of the dipole moment P_x (scalar) is normalized so that the obtained power values for a dipole located at large distance from the spheroid is equal to those values obtained from planewave irradiation. Since the far-field radiated power is inversely proportional to the square of the distance from the spheroid, it is necessary to adjust the value of the normalization constant in proportion to the square of the distance.

This is because any meaningful comparison between the dipole and planewave irradiation cases should involve a distance dependent normalization constant so as to maintain equal radiation powers in both cases. Therefore the resulting differences (if any) can be attributed to the reactive energy existing at short separation distances from the dipole. The normalization procedure simply involves equating the energy flux of the dipole source entering a solid angle subtended by the spheroid and the total planewave energy crossing the maximum cross-sectional area of the spheroid perpendicular to the direction of propagation. The energy flux is obtained by integrating the normal component of the Poynting vector of the dipole over the solid angle while the planewave energy is calculated by multiplying the incident power density (e.g., 1 mW/cm^2) by the area πb^2, where b is the semiminor axis of the spheroid. It is clear that this normalization constant is introduced only to scale the power values, but has no effect on the relative distribution.

The power distribution in a spheroidal model of man is shown in Fig. 2 for three different separation distances d.

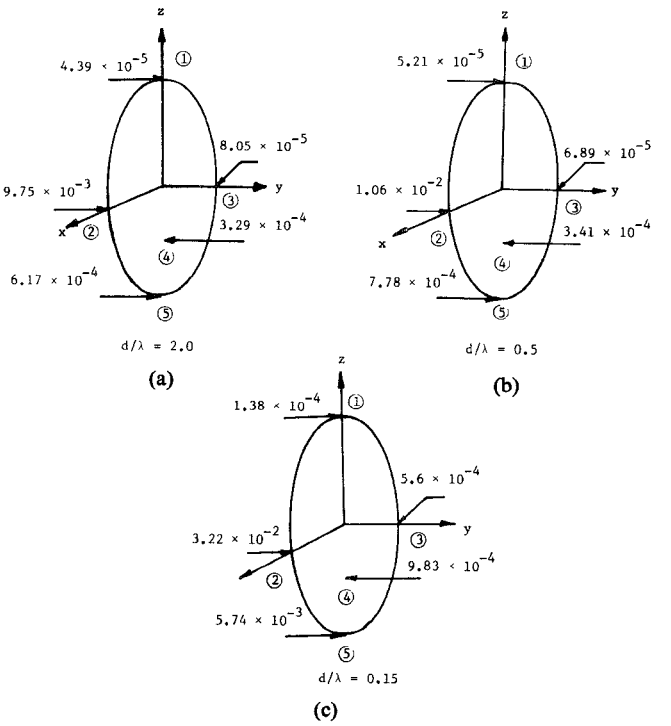

Fig. 2. SAR distribution at 27 MHz as a function of dipole location. $\bar{P}=P_x$ and $\theta=\pi$. (a) $d/\lambda=2$. (b) $d/\lambda=0.5$. (c) $d/\lambda=0.15$. The indicated locations (r,θ,ϕ) are: ① $(a,0,0)$, ② $(b,\pi/2,0)$, ③ $(b,\pi/2,\pi/2)$, ④ $(a/2,\pi,0)$, and ⑤ $(a,\pi,0)$.

TABLE II
COMPARISON BETWEEN THE PLANEWAVE (E-POLARIZATION [1]) SAR DISTRIBUTION IN A SPHEROIDAL MODEL OF MAN AT 27 MHz AND THE CORRESPONDING VALUES OBTAINED WHEN THE SAME MODEL IS IRRADIATED BY THE FIELDS OF A SHORT ELECTRIC DIPOLE OF MOMENT IN THE z-DIRECTION $\bar{P}=P_z$ AND LOCATED AT $\theta=\pi/2$ AND DISTANCE $d=2\lambda$; THE SAR DISTRIBUTION IS SYMMETRICAL WITH RESPECT TO THE $\theta=\pi/2$ PLANE

Point Location (r, θ, φ)	SAR (W/kg)	
	Plane Wave	Short Electric Dipole
(a, 0, 0)	1.47×10^{-2}	1.45×10^{-2}
(a/2, 0, 0)	1.63×10^{-2}	1.61×10^{-2}
(b, π/2, 0)	4.73×10^{-2}	4.72×10^{-2}
(b, π/2, π/2)	1.45×10^{-2}	1.42×10^{-2}

While the distribution at large d is similar to that of the planewave case, significant variation in the power distribution is observed for smaller d. It is also shown that for very small values of d (Fig. 2(c)), the relative power values at both ends of the spheroid are about 40 compared with the ratio of 15 in the planewave irradiation case.

Second, we considered a dipole located at the $\phi=0$ plane and $\theta=90°$. If we assumed the dipole moment to be along the z direction, this irradiation condition will correspond at large d to the case of E-polarized incident planewave [1]. Comparison between results obtained for large d and the planewave case are given in Table II. In this case a normalization constant similar to that used in

the k polarization was also employed to scale the value of the dipole moment P_z. The power distribution as a function of the distance d is shown in Fig. 3. It is clear that the calculations showed little change in the power distribution for a dipole located at distances greater than 0.5 λ. This can be explained by considering a separate calculation of the relative ratio between the reactive and radiation energy of a small dipole. From the numerical values of this ratio, shown in Fig. 4, it is clear that for an inefficient source like a short electric dipole, the reactive energy is almost negligible compared to the radiation energy at distances larger than $\lambda/2$.

The average SAR for the spheroidal model of man is also calculated as a function of the separation distance for the $\bar{P}=P_z$ and $\theta=90°$ case. These results are calculated by integrating the power distribution over the whole volume of the spheroidal and taking advantage of the symmetry consideration whenever possible. It should be noted that the procedure which involves the extinction and scattering cross sections to calculate the absorbed power by the spheroid is not adequate in the near-field calculations. This is because the basic definitions involved in this procedure are only applicable for planewave irradiation and not for the near field [5].

IV. Discussion and Conclusions

The power distribution in and the average SAR values of a prolate spheroidal model of man irradiated in the near field of a short dipole are presented. Results for dipoles parallel to the major axis and located at $\theta=90°$ (E polarization) and for dipoles parallel to the x axis and located at $\theta=180°$ (k polarization) are presented. It is shown that while large variation in the power distribution may result from the reactive energy components at smaller distances from the dipole, the average SAR values oscillate around the constant value obtained from the planewave irradiation. In an attempt to verify these results experimentally [16], the radiation fields of a short electric dipole were mapped as a function of distance. It is shown that the vector electric field is dominated in the far-field region ($d/\lambda>0.5$) by the component parallel to the dipole axis (E_θ) in the $\theta=\pi/2$ plane. In the near-field region, however, the vector electric field was found to be dominated by the component perpendicular to the dipole axis (E_r) in the plane $\theta=\pi/2$. Based on the absorption characteristics given in [1], it can be shown that the internal fields induced inside the spheroidal model are stronger when the incident field is mostly parallel to the major axis of the spheroid, and weaker when the incident field is mostly perpendicular to the major axis. Thus by combining the above experimental observations and absorption characteristics, the reduction in the average SAR given in Fig. 5 in the region between $0.17<d/\lambda<0.32$ can be explained. The steady increase in the average SAR for $d/\lambda<0.17$, however, is due to the strong reactive near-field components, the matter which compensates for the reductions as a result of the change in the direction of the vector electric field as explained above [16].

Also of particular interest is the high-power concentration near the tip of the spheroidal model in the k-polariza-

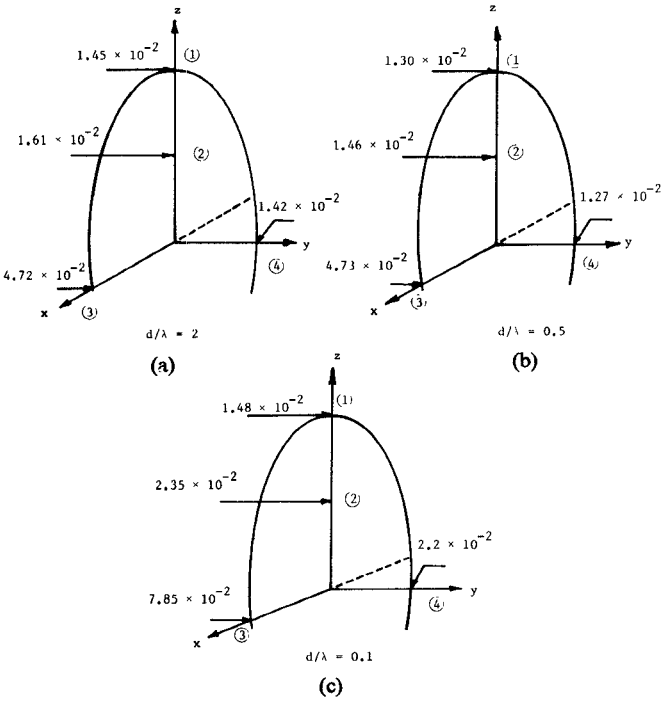

Fig. 3. SAR (W/kg) distribution at 27 MHz as a function of dipole location. $\bar{P}=P_z$ and $\theta=\pi/2$. (a) $d/\lambda=2$. (b) $d/\lambda=0.5$. (c) $d/\lambda=0.1$. The indicated locations (r,θ,ϕ) are: ① $(a,0,0)$, ② $(a/2,0,0)$, ③ $(b,\pi/2,0)$, and ④ $(b,\pi/2,\pi/2)$.

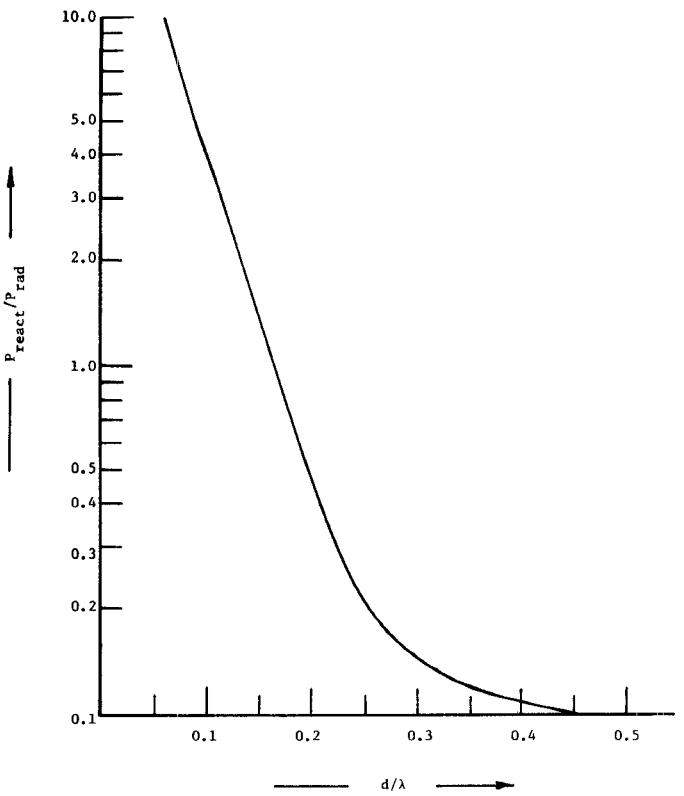

Fig. 4. The ratio between the total reactive power (P_{react}) and the radiation power (P_{rad}) of a current element (short dipole) at 27 MHz.

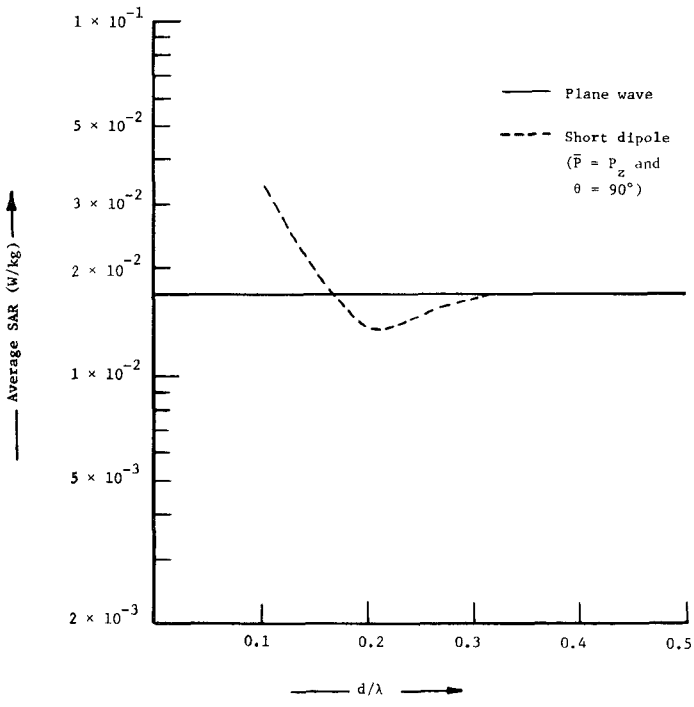

Fig. 5. Average SAR (W/kg) values at 27 MHz of a prolate spheroidal model of man as a function of the dipole location. $\bar{P}=P_z$ and $\theta=\pi/2$.

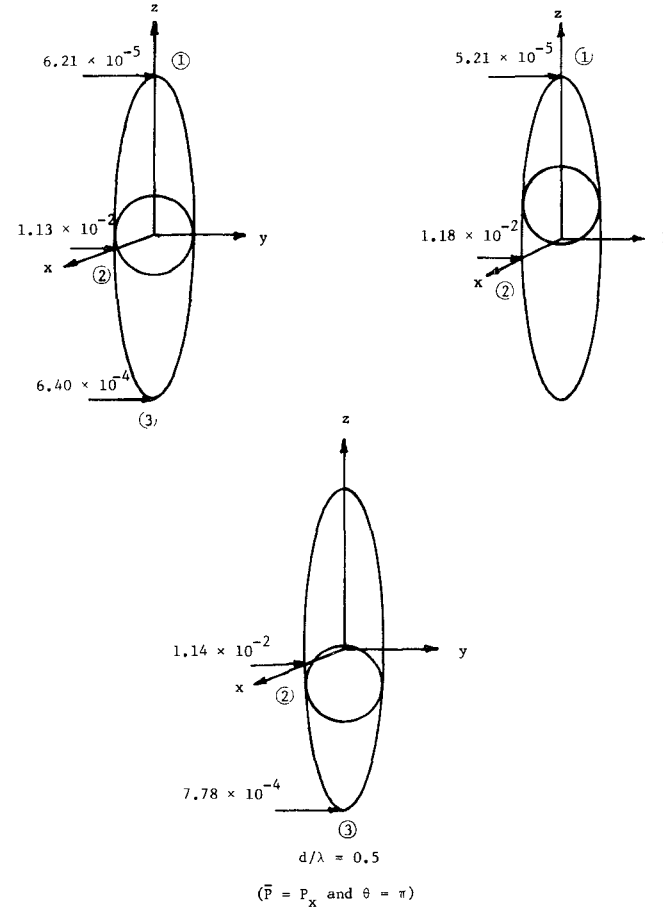

Fig. 6. Convergence of the solution at the ends of the spheroidal as obtained by shifting the origin of the inscribed sphere. The indicated locations (r,θ,ϕ) are: ① $(a,0,0)$, ② $(b,\pi/2,0)$, and ③ $(a,\pi,0)$.

tion case as it approaches the dipole source. This result simply suggests the possible enhancement of the near-field absorption in regions of small radius of curvature. It should be noted that the oscillation of the average SAR values for the E-polarization case and the possible enhancement of the near-field absorption in regions of small radius of curvature are general characteristics and expected to be valid for the other spheroidal models of different dimensions at frequencies below the resonance frequency [16]. The magnitudes of these changes, however, will obviously depend on the typical dimensions of the model and the exposure frequency. In summary, the results presented in this paper simply emphasize the importance of identifying the direction as well as the magnitude of the incident radiation if a meaningful evaluation of the possible hazards due to near-field exposure is to be made.

The numerical calculations presented, however, are certainly more involved and cumbersome compared to those of the planewave irradiation. The basic subroutines employed in the computer program in both cases are the same; however, larger matrices are generally required for the solution to converge in the near-field irradiation case.

In particular, the matrix size for a given frequency continued to increase with the decrease of the separation distance simply because the reactive energy components require more terms to be accurately calculated using (4). Furthermore, the straightforward solution given in (7) and (8) failed to provide convergent results for dipoles located at very small distances d. This is because (1) is constructed by equating the fields equal to zero inside a sphere of radius equal to the minor semiaxis of the spheroid. Therefore, the obtained results are expected to converge in the section bounded by the inscribed sphere and continue to be less accurate as the distance of the observation point from the center of the sphere increases. Obviously the inaccurate results will first appear at the spheroidal ends since these points have the largest distance from the center of the sphere at $z=0$. The procedure described by Waterman [10], however, assures a convergent solution by using the analytical continuation throughout the entire internal volume of the spheroid. Therefore, if the center of the internal sphere is continuously shifted along the z axis so as to maintain relatively short distances from the observation point to the center of a given sphere, a convergent solution in each section can be obtained sequentially. The procedure is illustrated in Fig. 6 where a convergent solution of the upper and lower halves of the spheroids are obtained by shifting the origin to $z=+a/4$ and $z=-a/4$, respectively. It should be noted that accurate values are obtained only in the middle section of the spheroid when a sphere with origin at $z=0$ is used.

Acknowledgment

The authors wish to thank the reviewers for their critical review of the manuscript and valuable suggestions.

REFERENCES

[1] C. H. Durney, C. C. Johnson, P. W. Barber, H. Massoudi, M. F. Iskander, J. L. Lords, D. K. Ryser, S. J. Allen, and J. C. Mitchell, *Radiofrequency Radiation Dosimetry Handbook* 2nd ed., Departments of Electrical Engineering and Bioengineering, University of Utah, Salt Lake City, UT, 1978.

[2] C. C. Johnson, C. H. Durney, and H. Massoudi, "Long-wavelength electromagnetic power absorption in prolate spheroidal models of man and animals," *IEEE Trans. Microwave Theory Tech.*, vol. MTT-23, pp. 739–747, Sept. 1975.

[3] C. H. Durney, C. C. Johnson, and H. Massoudi, "Long-wavelength analysis of plane wave irradiation of a prolate spheroid model of man," *IEEE Trans. Microwave Theory Tech.*, vol. MTT-23, pp. 246–254, Feb. 1975.

[4] H. Massoudi, C. H. Durney, and C. C. Johnson, "Long-wavelength electromagnetic power absorption in ellipsoidal models of man and animals," *IEEE Trans. Microwave Theory Tech.*, vol. MTT-25, pp. 47–52, Jan. 1977.

[5] P. W. Barber, "Resonance electromagnetic absorption by nonspherical dielectric objects," *IEEE Trans. Microwave Theory Tech.*, vol. MTT-25, pp. 373–381, May 1977.

[6] O. P. Gandhi, "Conditions of strongest electromagnetic power deposition in man and animals," *IEEE Trans. Microwave Theory Tech.*, vol. MTT-23, pp. 1021–1029, Dec. 1975.

[7] A. W. Guy, J. F. Lehmann, and J. B. Stonebridge, "Therapeutic applications of electromagnetic power," *Proc. IEEE*, vol. 62, pp. 55–75, 1974.

[8] D. L. Conover, W. H. Parr, E. L. Sensintaffar, and W. E. Murray, Jr., *Measurement of Electric and Magnetic Field Strengths from Industrial Radiofrequency (15-40.68 MHz) Power Sources*, C. C. Johnson and M. L. Shore, Eds., HEW Publication (FDA) 77-8011, Dec. 1976.

[9] P. F. Wacker and R. R. Bowman, "Quantifying hazardous electromagnetic fields: Scientific basis and practical considerations," *IEEE Trans. Microwave Theory Tech.*, vol. MTT-19, pp. 178–187, Feb. 1971.

[10] P. C. Waterman, "Symmetry, unitary, and geometry in electromagnetic scattering," *Phys. Rev. D.*, vol. 3, pp. 825–839, 1971.

[11] P. W. Barber and C. Yeh, "Scattering of electromagnetic waves by arbitrary shaped dielectric bodies," *Appl. Opt.*, vol. 14, 1975, pp. 2864–2872.

[12] J. D. Jackson, *Classical Electrodynamics*. New York: Wiley, 1962.

[13] A. Hizal and Y. K. Baykal, "Heat potential distribution in an inhomogeneous spherical model of a cranial structure exposed to microwaves due to loop or dipole antennas," *IEEE Trans. Microwave Theory Tech.*, vol. MTT-26, pp. 607–612, Aug. 1978.

[14] H. Chew, P. J. McNutly, and M. Kerker, "Model for raman and fluorescent scattering by molecules embedded in small particles," *Phys. Rev. A.*, vol. 13, 1976, pp. 396–404.

[15] P. M. Morse and H. Feshbach, *Methods of Theoretical Physics*. New York: McGraw-Hill, 1953.

[16] M. F. Iskander, H. Massoudi, C. H. Durney, and S. J. Allen, "Measurements of the RF power absorption in human and animal phantoms exposed to near-field radiation," to be published.

Short Paper

A General Equivalent Network of the Input Impedance of Symmetric Three-Port Circulators

G. BITTAR AND GY. VESZELY

***Abstract*—Starting from the network model of ferrite-filled resonators, a general equivalent network of the input impedance of symmetric, three-port circulators is given. The main advantage of the network, that it contains the original elements of the resonator model, so the physics of operation can be clearly seen and the results of field analysis can be directly used.**

I. THE NETWORK MODEL OF FERRITE-FILLED RESONATORS

Hammer [1] gave the network model of ferrite-filled resonators. If the resonator has a three-fold symmetry axis, the excitations are on magnetic wall and only two resonator modes are taken into account, then the network model can be seen in Fig. 1. The two ports marked by φ are nonreciprocal phase shifters. They have the characteristic as follows:

$$I_1 = -e^{-j\varphi} I_2,\ U_1 = e^{-j\varphi} U_2,\ \varphi = 0, \qquad \pm 2\pi/3. \tag{1}$$

The values of Z_r^+, Z_r^- can be obtained from the eigenvalues and losses of the resonator, and the transformer ratio T is obtainable from the eigenfunctions of the resonator and those of the coupling transmission lines [1]. The impedance matrix of the three port in Fig. 1 is

$$Z = \begin{bmatrix} Z_1 & Z_2 & Z_3 \\ Z_3 & Z_1 & Z_2 \\ Z_2 & Z_3 & Z_1 \end{bmatrix} \tag{2}$$

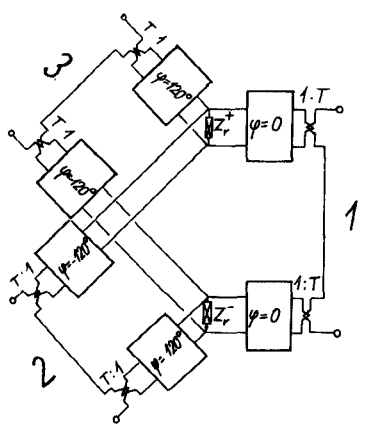

Fig. 1. The resonator model.

Manuscript received August 8, 1979; revised January 24, 1980.

The authors are with the Department of Theoretical Electricity, Technical University, 1521 Budapest, Hungary.

0018-9480/80/0700-0807$00.75 ©1980 IEEE